This is the accepted manuscript made available via CHORUS. The article has been published as:

# Preparation of Low Entropy Correlated Many-Body States via Conformal Cooling Quenches

Michael P. Zaletel, Adam Kaufman, Dan M. Stamper-Kurn, and Norman Y. Yao

Phys. Rev. Lett. **126**, 103401 — Published 10 March 2021

DOI: 10.1103/PhysRevLett.126.103401

# Preparation of Low Entropy Correlated Many-body States via Conformal Cooling Quenches

Michael P. Zaletel[1], Adam Kaufman[2], Dan M. Stamper-Kurn[1], Norman Y. Yao[1]
[1]*Department of Physics, University of California Berkeley, Berkeley, CA 94720, U.S.A. and*
[2]*JILA, University of Colorado and National Institute of Standards and Technology, and Department of Physics, University of Colorado, Boulder, Colorado 80309, U.S.A.*
(Dated: January 19, 2021)

We propose and analyze a method for preparing low-entropy many-body states in isolated quantum optical systems of atoms, ions and molecules. Our approach is based upon shifting entropy between different regions of a system by spatially modulating the magnitude of the effective Hamiltonian. We conduct two case studies, on a topological spin chain and the spinful fermionic Hubbard model, focusing on the key question: can a "conformal cooling quench" remove sufficient entropy within experimentally accessible timescales? Finite temperature, time-dependent matrix product state calculations reveal that even moderately sized "bath" regions can remove enough energy and entropy density to expose coherent low temperature physics. The protocol is particularly natural in systems with long-range interactions such lattice-trapped polar molecules and Rydberg-excited atoms where the magnitude of the Hamiltonian scales directly with the interparticle spacing. To this end, we propose simple, near-term implementations of conformal cooling quenches in systems of atoms or molecules, where signatures of low-temperature phases may be observed.

Ultracold quantum gases have reached the extraordinary realm of sub-nanokelvin temperatures [1, 2], revealing, along the way, phenomena ranging from Bose-Einstein condensation and Cooper-paired superfluidity to Mott insulators and localization [3–7]. This scientific impact owes, in part, to a flexible array of cooling techniques that can effectively quench the kinetic energy of atomic systems; indeed, the laser cooling of atomic registers in optical tweezers has enabled the observation of few-particle quantum interference and entanglement [8, 9], while the evaporative cooling of Bose gases has realized temperatures nearly two orders of magnitude smaller than that required for condensation [10].

Nevertheless, these temperatures are still too high to emulate a number of more exotic- and delicate- quantum phases including antiferromagnetic spin liquids, fractional Chern insulators and high-temperature superconductors [11–13]. The figure of merit for observing such physics is not the absolute temperature, but rather the dimensionless entropy density in units of $k_B$ [14]. Reaching ultra-low entropy densities remains a major challenge for many-body quantum simulations despite the multitude of kinetic cooling techniques. This challenge is particularly acute for gases in deep optical lattice potentials, for which transport, and thus evaporative cooling, is slowed [15]. Moreover, in lattice systems representing models of quantum magnetism, the entropy resides primarily in spin, rather than motional, degrees of freedom [16]. Expelling such entropy through evaporative cooling requires the conversion of spin excitations to kinetic excitations, a process that is typically inefficient [17–19].

To access low-entropy phases of matter, two broad approaches have been proposed toward overcoming this challenge. The first is adiabatic preparation, where one initializes a low entropy state and changes the Hamiltonian gradually until the desired many-body state is reached [20–22]. However, the final entropy density is bounded from below by the initial entropy density, and experimental constraints or phase transitions may preclude a suitable adiabat. The second approach is to 'shift entropy elsewhere' [11, 22–26], using the system's own degrees of freedom as a bath [17, 27, 28]. Recently, this technique has enabled the experimental observation of long-range antiferromagnetism in quantum simulations of the Fermi-Hubbard model.

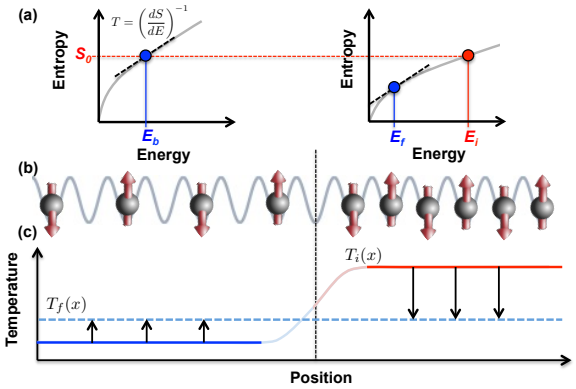


FIG. 1. a) If the Hamiltonian in the "bath" region is related to the Hamiltonian in the "system" region by a constant rescaling, $H_B = \lambda H_S$, their entropy-energy-density curves satisfy $s_B(E) = s_S(E/\lambda)$. Thus preparing at state with constant entropy density establishes a temperature differential $T_B = \lambda T_S$, since $T = \frac{dE}{dS}$. b) Schematic representation of trapped polar molecules interacting through a long-range dipolar $1/R_{ij}^3$ potential. If the interparticle spacing between the molecules on the left ("bath") is increased by a factor $d$ relative to the right ("system"), then $H_B = (\frac{1}{d})^3 H_S$ [29]. c) In this case, a uniform Neél state has a temperature differential after reaching local equilibrium, and the resulting evolution will remove entropy from the right half of the chain as the system reaches global equilibrium.

In this work, we propose and analyze a class of methods—termed 'conformal cooling quenches'—for shifting entropy by spatially modulating the *magnitude* of the Hamiltonian [30]. The intuition behind this approach is best illustrated as follows: Suppose that we take a system's Hamiltonian $H$ and either suddenly or adiabatically reduce it by a

factor $\lambda < 1$, taking $H \to \lambda H$. Since $k_B T$ has units of energy, the temperature $T$ is accordingly reduced by $T \to \lambda T$. When applied to the entire system, this "cooling" is trivial, since it amounts to a change of units without reducing the entropy density. However, if the reduction by $\lambda$ instead occurs for only a *portion* of the system, which we call the 'bath,' the change in temperature is physical, and establishes a temperature gradient; during equilibration, entropy will then flow out of the system and into the bath.

This generalizes previous studies, where entropy flow relies on particle itinerance, while the temperature gradient is inherited from a density gradient [22, 25, 26]. In particular, our method is applicable not only to itinerant Hubbard systems, but also to spin models. This latter case is especially relevant to recent developments in trapped ion arrays [31, 32], optical tweezer arrays [33, 34], and ultracold molecules [35, 36], where versatile spin models with spatially tunable Hamiltonian parameters are increasingly accessible.

One virtue of the conformal cooling approach is that it can "cool" a system within a metastable state-space. For example, conformal cooling can be applied to a gas equilibrating at negative kinetic or spin temperature [37], bringing the system toward zero temperature from below. It can also be applied to gases equilibrating in high-energy manifolds of states, i.e. in excited bands of an optical lattice [38, 39]. Systems equilibrating at negative temperatures or in higher bands can exhibit strong frustration without complicated band engineering.

We will begin by introducing the thermodynamics of our approach, focusing on two questions: 1) how much entropy can a cooling quench remove and 2) how long does it take? Next, we perform a large-scale numerical study of both a 1D topological spin-chain and the fermionic Hubbard model, demonstrating that realistic cooling quenches can remove enough entropy to reveal their low-temperature physics. Finally, we discuss natural experimental implementations of our approach focusing on ultracold polar molecules and Rydberg atom arrays.

*General Strategy*—We envision spatially demarcating the degrees of freedom into a "bath" (B) and "system" (S) which are placed "end-to-end," so that the coupling between their boundaries scales sub-extensively with their volume (Fig. 1b) [40]. We assume that the Hamiltonian $H_B$ (bath) is identical to $H_S$ (system), except that its magnitude is scaled by a factor $\lambda < 1$. The entropy ($s$) versus energy density ($E$) curves in the two regions are then related by $s_B(E) = s_S(E/\lambda)$ and their temperatures by $T_B(E) = \lambda T_S(E/\lambda)$ (Fig. 1a). In the following, we will consider two protocols, "quenched" and "adiabatic."

*Quench Protocol*—In the quench approach, the Hamiltonians are time-independent with $H_B = \lambda H_S$. At $t = 0$, we prepare a uniform initial state (e.g. a product state) and simply let it evolve. Equivalently, one can begin in thermal equilibrium with $H_B = H_S$, and then suddenly reduce $H_B$ to $H_B = \lambda H_S$. The overall system is now in *local* equilibrium, with the local density matrices in $B$ and $S$ identical, and thus, $s_B = s_S$ and $T_B = \lambda T_S$. As the system evolves toward

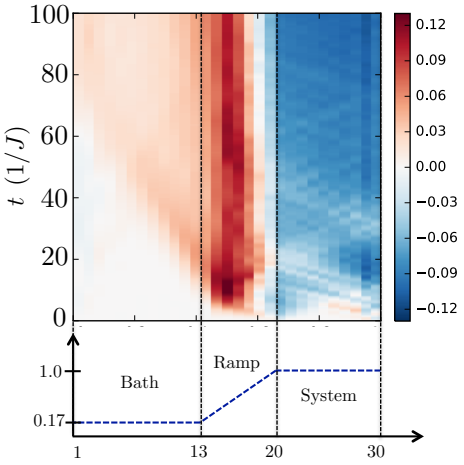


FIG. 2. 'Quench' cooling of a 30-site spin-1 Haldane chain. After initializing the state at $t = 0$ with uniform entropy density, the coupling constants $\lambda_x$ are scaled according to the bottom panel, which should transport heat from the 'system' on the right to the 'bath' on the left. In the top panel, we plot the change in energy density $h_x(t) - h_x(0)$ as the chain evolves.

*global* equilibrium, entropy will follow the thermal gradient and flow from $S$ to $B$.

The final equilibrium temperature $T_{\rm f}^{(q)}$ is determined by energy conservation post-quench. Noting that the energy just after the quench is $N_S E_S(T_i) + N_B \lambda E_S(T_i)$, and using the relation $E_B(T) = \lambda E_S(T/\lambda)$, we have:

$$(N_S + \lambda N_B) E_S(T_{\rm i}) = N_S E_S(T_{\rm f}^{(q)}) + N_B \lambda E_S(T_{\rm f}^{(q)}/\lambda), \tag{1}$$

where $N_S, N_B$ are the number of sites in the system and bath, and $T_{\rm i}$ is the initial temperature of the system. When $\lambda N_B \gg N_S$, we have $T_{\rm f}^{(q)} = \lambda T_i$, but more generally one should choose $\lambda$ so as to minimize $T_{\rm f}^{(q)}$ based on the precise form of $E_S(T)$. While we have assumed a sharp distinction between $S$ and $B$ for simplicity, one can let the spatial modulation $\lambda(\vec{x})$ vary smoothly, for example in the "ramp" region shown in Figs. 2 and 4(a), in which case Eq. (1) is replaced by an integral over the energy density.

*Adiabatic Protocol*—The cooling is more effective if the magnitude of $H_B = \Lambda(t) H_S$ is instead slowly reduced in time, with $\Lambda(t = 0) = 1$ and $\Lambda(t \to \infty) = \lambda$. In the isentropic limit, the final system temperature $T_{\rm f}^{(a)}$ is determined by

$$(N_B + N_S) s_S(T_{\rm i}) = N_B s_S(T_{\rm f}^{(a)}/\lambda) + N_S s_S(T_{\rm f}^{(a)}), \tag{2}$$

with $T_{\rm f}^{(a)} \leq T_{\rm f}^{(q)}$. When the bath and system are end-to-end, diffusive dynamics imply that the equilibration time, $t_{\rm eq}$, scales as $L_S^2/\Lambda(t)$ (q.v. Eq. (4)) where $L_S$ is the linear extent of the system and adiabaticity requires $\partial_t \Lambda \ll 1/t_{\rm eq}$. For small $\Lambda$, the bath and system will eventually fall out of equilibrium and additional entropy will be produced, though the temperature will always be upper-bounded by $T_{\rm f}^{(q)}$.

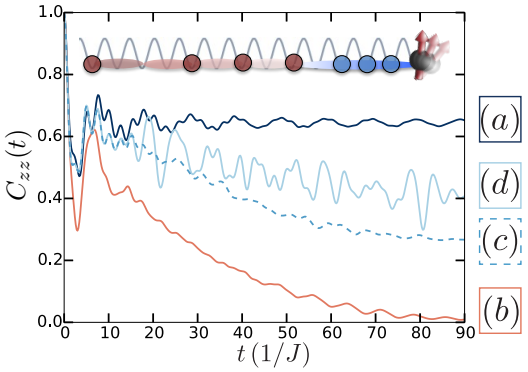


FIG. 3. The dynamical correlation function, $C_{zz}(t)$, measured after four initialization protocols: a) Optimal: $C_{zz}(t)$ for the ground state of an $L = 10$ chain; b) finite $T = 0.51J$, without a cooling quench. The edge coherence rapidly decays. c) finite $T_i = 0.51J$, but starting the $C_{zz}$ measurement after the cooling quench shown in Fig. 2. The coherence is improved by an order of magnitude. d) Same as (c), but eliminating the coupling between sites $i = 20$ and 21 after the quench, which cuts off the bath.

To demonstrate that conformal cooling can shift significant entropy out of the system even for moderate bath sizes and short time-scales, we numerically investigate two distinct settings: the $S = 1$ Haldane topological anti-ferromagnet and the fermionic Hubbard model.

*Conformal cooling in an $S = 1$ Haldane chain*—Consider a one dimensional chain of $S = 1$ spins with Hamiltonian

$$H[\lambda_x] = \sum_x \lambda_x h_x = J \sum_x \lambda_x \left[ \mathbf{S}_x \cdot \mathbf{S}_{x+1} + \frac{\gamma}{3} (\mathbf{S}_x \cdot \mathbf{S}_{x+1})^2 \right]. \tag{3}$$

At both the Heisenberg point $\gamma = 0$ and the AKLT point $\gamma = 1$, the spin-chain is a gapped topological paramagnet in the Haldane phase [41, 42]. The topology of the phase has a striking signature in a finite-length chain, which exhibits a pair of localized spin-1/2 edge states. At temperatures below the bulk gap, $T < \Delta \sim J$, these localized edge states can coherently store quantum information for long times, providing a sharp experimental signature of the topological phase [43].

Calculating the thermodynamic energy-temperature relation, $E(T)$, using exact diagonalization reveals that a modest bath size of $N_B/N_S \approx$ 2-3 is sufficient to cool from the Neél product state $|\uparrow\downarrow\uparrow\downarrow\cdots\rangle$, which corresponds to an initial temperature $T_{\rm i} = 1.45\Delta$, to well below the gap, $T_{\rm f}^{(q)} \approx 0.7\Delta$ [44]. Here the pure-state temperature is defined by inverting $E(T)$. Since the spin chain is diffusive [45], the timescale required for cooling is determined by Fourier's law. When $\lambda(x)$ varies smoothly compared to the lattice scale, the local thermal conductivity $\kappa$ and specific heat $c$ are determined by rescaling, $\kappa(T, x) = \lambda(x)\kappa_S(T(x)/\lambda(x))$ and $c(T, x) = c_S(T(x)/\lambda(x))$, where $\kappa_S(T)$ and $c_S(T)$ are defined with $\lambda = 1$. Applying this within a simple lumped element model predicts that temperature will decrease as [44],

$$T_S(t) \sim T_{\rm f}^{(q)} + \mathcal{K} \frac{L_S}{\sqrt{t D_B}} (T_{\rm i} - T_{\rm f}^{(q)}) \tag{4}$$

where $D_B$ is the thermal diffusivity of the bath and $\mathcal{K}$ is an $\mathcal{O}(1)$ geometrical factor. For bath temperatures above $\lambda J$, the diffusivity will generically saturate to a temperature-independent value, $D_B \propto \lambda J/\hbar$ [46], implying that $t_{\rm eq} \sim L_S^2 (\lambda J/\hbar)^{-1}$.

To verify these dynamics, we simulate the evolution of a finite-energy density pure state using the TEBD-algorithm [47]. It is exponentially difficult to simulate finite temperature dynamics and our simulations require an MPS bond-dimension of $m = 20,000$, limiting our system to $L = 30$ sites (Fig. 2) [48]. We initialize a uniform state $|\Psi(0)\rangle = e^{-\tau \hat{H}[\lambda_x = 1]} |\uparrow\downarrow\uparrow\downarrow\cdots\rangle$, where $\tau = 0.35/J$, resulting in an energy density that corresponds to temperature $T_S = 0.51J$ after local equilibration [49]. The system is then quenched into a spatially non-uniform $\hat{H}[\lambda_x]$ (Fig. 2). Using the optimal $\lambda_0 = 0.17$ in the 'bath' leads to a final predicted temperature: $T_{\rm f}^{(q)} = 0.29J$.

The evolution of the local energy density $\langle \lambda_x \hat{h}_x(t) \rangle$ during the cooling quench is depicted in Fig. 2. The energy density in region $S$ at time $t = 100/J$ corresponds to $T_S = 0.34J$, within 14% of the expected $T_{\rm f}^{(q)}$ [44]. Moreover, the relaxation dynamics are roughly consistent with $T_S \sim T_{\rm f}^{(q)} + (T_{\rm i} - T_{\rm f}^{(q)})\sqrt{t_{\rm eq}/t}$, where $t_{\rm eq} \approx 0.22(\mathcal{K} L_S)^2 (\lambda J/\hbar)^{-1}$, consistent with the expectation $1/D_B \sim 0.19/\lambda$ [44, 46].

Even for a relatively small bath size, the cooling quench has a dramatic effect on the dynamical correlation function of the topological edge mode. Since the edge state in region $S$ will generically have overlap with the right-most spin $S^{\mu}_{\rm end}$, its coherence can be probed via the correlation function

$$C_{zz}(t) = \langle \Psi | \, S^z_{\rm end}(t + t_f) S^z_{\rm end}(t_f) \, | \Psi \rangle \,, \tag{5}$$

where the measurement only begins after the cooling quench is complete ($t_f = 100/J$). At $T = 0$, these correlations should asymptote to a finite constant [Fig. 3a], while at large $T$ [Fig. 3d], they will decay exponentially. We compare $C_{zz}(t)$ under four preparation scenarios described in Fig. 3. The conformal cooling quench improves the coherence time (i.e. the decay timescale of $C_{zz}(t)$) by more than an order of magnitude.

*Adiabatic conformal cooling in the fermionic Hubbard model*—We next consider the adiabatic protocol applied to the fermionic Hubbard model, $H = -\sum_{<i,j>,\sigma} t_{ij} c^{\dagger}_{i\sigma} c_{j\sigma} + U \sum_i n_{i\uparrow} n_{i\downarrow} - \mu \sum_{i\sigma} n_{i\sigma}$. Here, we focus on the Mott insulating phase at half-filling with $t/U \ll 1$ and $T < U$. While the fermions' motion is quenched, their spins interact via an effective anti-ferromagnetic Heisenberg interaction, $H_{\rm eff} = \sum_{\langle i,j \rangle} J_{ij} [\mathbf{S}_i \cdot \mathbf{S}_j - \frac{1}{4}]$, where $J = 4\frac{t_{ij}^2}{U}$ is the super-exchange coupling.

In the Mott regime where the dynamics are governed by $H_{\rm eff}$, adiabatic cooling is naturally realized by decreasing $J$

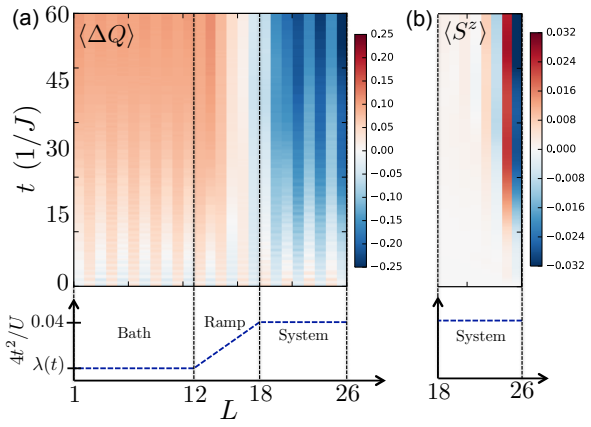


FIG. 4. Cooling dynamics in the 1D spinful Hubbard model. a) After initializing a $T = 1.4J$ thermal state with uniform Hamiltonian $U = 1, t_{ij} = 0.1$, the hopping $t_{ij}$ is adiabatically decreased with a spatial profile shown in the bottom panel. The top panel shows the change in the heat density as a function of time. b) Depicts the onset of antiferromagnetic correlations. The right-most site has a small Zeeman field $0.05S^z$. While the initial temperature disorders the spins, as the system cools, algebraic anti-ferromagnetic correlations clearly emerge.

in the bath region (relative to the system region); one can achieve this by weakly modulating the depth of the optical potential, $V(\vec{x}) = -V_0(\vec{x}) \sum_{i=1}^{d} \cos(k\, x^i)^2$, where $V_0(\vec{x})$ is slowly varying and $k$ is the wavevector of optical lattice. Increasing $V_0$ has three effects on the effective Hamiltonian: $U$ will increase, as the orbitals are further localized, $\mu$ will increase, as the trap is deeper and $t$ will decrease due to the barrier height. Since $t$ is exponentially more sensitive than $U$ to the trap-depth, $\xi = \sqrt{\frac{V_0}{E_r}}$ ($E_r$ is the recoil energy), the dominant effect is to modulate the hoppings [50]. Assuming $\mu$ is compensated to maintain half-filling, the super-exchange energy becomes $J_{ij} \propto \xi^2(x) e^{-4\xi(x)}$, precisely the desired modulation. Fortuitously, a small modulation in $V_0$ is already capable of dramatically reducing the system's temperature; for example, in the the 3D cubic Heisenberg model, a 6% change in the lattice depth can cool the system from $1.4T_{\rm N}$ [51] down to the Néel temperature, $T_{\rm N}$ [44].

Note that in the above approach, we choose to scale $t$ but not $U$, which differs from the overall scaling, $H \to \lambda H$, we had initially used to motivate our work. Of course in the limit $t, T \ll U$, the conclusions are the same because the thermodynamics are governed by $H_{\rm eff} \propto J = 4t^2/U$, so scaling $t$ does effectively enact an overall scaling of the Hamiltonian. But more generally, cooling only requires the criteria $\partial_t T(s; t, U) > 0$, which we have verified using determinantal quantum Monte Carlo [44], so long as the initial entropy density satisfies $s < k_B \log(2)$ [52]. To this end, our proposal will also work away from the $t, T \ll U$ limit.

To confirm the effectiveness of the adiabatic protocol, we simulate the dynamics of the spinful 1D fermionic Hubbard model. We use the TEBD method to time evolve a purified finite-temperature ensemble [53]. At time $t = 0$ the Hamiltonian is uniform, $U = 1, t_{ij} = 0.1$, with an initial thermal state $\rho = e^{-H/T_i}/\mathcal{Z}$ at $T_i = 1.4J$. We then time evolve the ensemble with a Hamiltonian, $H(t)$, in which $t_{ij}$ decreases adiabatically in the bath [44]. Since Hamiltonian changes in time, energy is not conserved, and we divide it into heat and work, $\dot{E} = \dot{Q} - \dot{W}$ [44], enabling us to plot the evolution of the heat-density $Q$ in Fig. 4(a). Total heat is conserved, but with clear transport from $S$ to $B$. As a more qualitative thermometer, we note that at $T = 0$, the system should display algebraic anti-ferromagnetic correlations. To reveal them, we place a small Zeeman field $H = 0.05S^z$ on the right edge spin, both in the initial thermal state and the subsequent dynamics. As depicted in Fig. 4(b), the finite temperature of the initial thermal state disorders the magnetization $\langle S^z \rangle$, but as the dynamics proceed and cooling occurs, the antiferromagnetic correlations become clearly manifest.

*Experimental implementation*—Our conformal cooling protocols are well suited to systems with long-ranged interactions, such as polar molecules, Rydberg atoms, and trapped ions [29, 54–57]. To implement the quench protocol, we envision a setup where the average spacing between particles is larger in the bath than in the system, $r_B > r_S$. Assuming power-law interactions ($1/R^\alpha$), the Hamiltonian in $B$ will be reduced by a constant factor $\lambda = (r_S/r_B)^\alpha$ relative to that in $S$ (Fig. 1b) [58].

This approach is particularly applicable to two classes of current generation experimental platforms: ultracold polar molecules and Rydberg atom arrays. In the molecular context, the optical lattice filling fraction, $\nu < 1$, leads to random dilution [29]. Fortunately, the cooling quench is natural to implement in this randomly diluted case, since one can make $r_B > r_S$ merely by modulating the average density, without having to ensure the particles in $B$ lie on a particular sub-lattice. In this case, simply time-evolving an initial product state in the presence of this density modulation will cool the high-density region, and could provide a simple route towards studying, for example, algebraically correlated random-singlet phases [59–61].

Although we have studied the AKLT model because it admits simple numerical observables for quantifying entropy, the same cooling protocol can also be applied to the long-range, mixed-field Ising model, which is naturally realized in a Rydberg atom array [33, 34, 62–64]. In this case, the spacing between the atoms and/or the intensity of the Rydberg excitation light, can be made spatially varying, in order to create well-defined bath and system regions in one, two, or even three-dimensions [65–67]. The complex phase diagram associated with this model exhibits a variety of competing orders and phase transitions, providing a rich playground for implementing conformal cooling [68].

In summary, we have proposed a general method for preparing low-entropy many-body states in isolated quantum systems. Our approach can be naturally implemented in systems with power law interactions by simply diluting the particle density of the bath region; moreover, in the supplemen-

tal materials, we also provide a simple experimental blueprint for implementing conformal cooling in the spinful fermionic Hubbard model [44]. Looking forward, our proposal raises a number of intriguing questions: is it possible to implement a refrigeration cycle by repeated preparation of the bath state? Can one optimize a side-by-side geometry which could reduce the equilibration time? By performing conformal cooling during a quantum phase transition, can one reduce the rate of Kibble-Zurek defect formation [62]?

We thank Randy Hulet, Jun Ye, and Martin Zwierlein for insightful suggestions and illuminating conversations. We acknowledge the QUEST-DQMC collaboration [69] for providing the code used in our QMC calculations. This work was supported by the ARO through the MURI program (W911NF-17-1-0323 and W911NF-20-1-0136), the President's Research Catalyst Award CA-15-327861 from the University of California Office of the President, the David and Lucile Packard foundation and the W. M. Keck foundation.

[1] A. Leanhardt, T. Pasquini, M. Saba, A. Schirotzek, Y. Shin, D. Kielpinski, D. Pritchard, and W. Ketterle, Science **301**, 1513 (2003).
[2] T. Kovachy, J. M. Hogan, A. Sugarbaker, S. M. Dickerson, C. A. Donnelly, C. Overstreet, and M. A. Kasevich, Phys. Rev. Lett. **114**, 143004 (2015).
[3] M. Anderson, J. Ensher, M. Matthews, C. Wieman, and E. Cornell, science **269**, 14 (1995).
[4] K. B. Davis, M.-O. Mewes, M. R. Andrews, N. Van Druten, D. Durfee, D. Kurn, and W. Ketterle, Phys. Rev. Lett. **75**, 3969 (1995).
[5] B. DeMarco and D. S. Jin, Science **285**, 1703 (1999).
[6] C. Chin, M. Bartenstein, A. Altmeyer, S. Riedl, S. Jochim, J. H. Denschlag, and R. Grimm, Science **305**, 1128 (2004).
[7] M. Schreiber, S. S. Hodgman, P. Bordia, H. P. Lüschen, M. H. Fischer, R. Vosk, E. Altman, U. Schneider, and I. Bloch, Science **349**, 842 (2015).
[8] A. M. Kaufman, B. J. Lester, and C. A. Regal, Physical Review X **2**, 041014 (2012).
[9] A. Kaufman, B. Lester, C. Reynolds, M. Wall, M. Foss-Feig, K. Hazzard, A. Rey, and C. Regal, Science **345**, 306 (2014).
[10] R. Olf, F. Fang, G. E. Marti, A. MacRae, and D. M. Stamper-Kurn, Nature Physics **11**, 720 (2015).
[11] D. M. Stamper-Kurn, Physics **2**, 80 (2009).
[12] G. Campbell, Nature **480**, 463 (2011).
[13] N. Y. Yao, A. V. Gorshkov, C. R. Laumann, A. M. Läuchli, J. Ye, and M. D. Lukin, Phys. Rev. Lett. **110**, 185302 (2013).
[14] Quantum Monte Carlo estimates for the entropy density required for magnetic ordering are: $\sim 0.03k_B$ and $\sim 0.3k_B$ for bosons in two- and three-dimensional lattices, respectively, with similar values for the Neel ordering of fermions. On the experimental front, spin gradient demagnetization of bosons has reached $\sim 0.05k_B$ [70], while evaporative cooling has reached $\sim 10^{-3}k_B$ [10]. For Fermions, $\sim 0.06k_B$ has been reached unitary Fermi gases [71], while $\sim 0.76k_B$ has been achieved in a 3D optical lattice [17]. Antiferromagnetic correlations have also been observed in a 2D Fermi-Hubbard model using quantum gas microscopy [18, 19].
[15] C.-L. Hung, X. Zhang, N. Gemelke, and C. Chin, Phys. Rev. Lett. **104**, 160403 (2010).
[16] S. Chu, Nature **416**, 206 (2002).
[17] R. A. Hart, P. M. Duarte, T.-L. Yang, X. Liu, T. Paiva, E. Khatami, R. T. Scalettar, N. Trivedi, D. A. Huse, and R. G. Hulet, Nature **519**, 211 (2015).
[18] M. F. Parsons, A. Mazurenko, C. S. Chiu, G. Ji, D. Greif, and M. Greiner, arXiv preprint arXiv:1605.02704 (2016).
[19] L. W. Cheuk, M. A. Nichols, K. R. Lawrence, M. Okan, H. Zhang, E. Khatami, N. Trivedi, T. Paiva, M. Rigol, and M. W. Zwierlein, arXiv preprint arXiv:1606.04089 (2016).
[20] A. S. Sørensen, E. Altman, M. Gullans, J. Porto, M. D. Lukin, and E. Demler, Physical Review A **81**, 061603 (2010).
[21] M. Barkeshli, N. Yao, and C. Laumann, Phys. Rev. Lett. **115**, 026802 (2015).
[22] C. S. Chiu, G. Ji, A. Mazurenko, D. Greif, and M. Greiner, Phys. Rev. Lett. **120**, 243201 (2018).
[23] J. Catani, G. Barontini, G. Lamporesi, F. Rabatti, G. Thalhammer, F. Minardi, S. Stringari, and M. Inguscio, Phys. Rev. Lett. **103**, 140401 (2009).
[24] D. Greif, G. Jotzu, M. Messer, R. Desbuquois, and T. Esslinger, Phys. Rev. Lett. **115**, 260401 (2015).
[25] A. Mazurenko, C. S. Chiu, G. Ji, M. F. Parsons, M. Kanász-Nagy, R. Schmidt, F. Grusdt, E. Demler, D. Greif, and M. Greiner, Nature **545**, 462 (2017).
[26] A. Kantian, S. Langer, and A. J. Daley, Phys. Rev. Lett. **120**, 060401 (2018).
[27] T. Paiva, Y. L. Loh, M. Randeria, R. T. Scalettar, and N. Trivedi, Phys. Rev. Lett. **107**, 086401 (2011).
[28] C. J. M. Mathy, D. A. Huse, and R. G. Hulet, Phys. Rev. A **86**, 023606 (2012).
[29] S. A. Moses, J. P. Covey, M. T. Miecnikowski, B. Yan, B. Gadway, J. Ye, and D. S. Jin, Science **350**, 659 (2015).
[30] A familiar example of such an approach is magnetic refrigeration, for which $H \sim \mathbf{B}(t) \cdot \mathbf{m}$, where $\mathbf{B}$ is an external magnetic field and $\mathbf{m}$ the magnetization [72, 73].
[31] J. W. Britton, B. C. Sawyer, A. C. Keith, C. C. J. Wang, J. K. Freericks, H. Uys, M. J. Biercuk, and J. J. Bollinger, Nature **484**, 489 (2012).
[32] J. Zhang, G. Pagano, P. W. Hess, A. Kyprianidis, P. Becker, H. Kaplan, A. V. Gorshkov, Z. X. Gong, and C. Monroe, Nature **551**, 601 (2017).
[33] H. Labuhn, D. Barredo, S. Ravets, S. de Léséleuc, T. Macrì, T. Lahaye, and A. Browaeys, Nature **534**, 667 EP (2016).
[34] H. Bernien, S. Schwartz, A. Keesling, H. Levine, A. Omran, H. Pichler, S. Choi, A. S. Zibrov, M. Endres, M. Greiner, V. Vuletić, and M. D. Lukin, Nature **551**, 579 EP (2017).
[35] B. Yan, S. A. Moses, B. Gadway, J. P. Covey, K. R. A. Hazzard, A. M. Rey, D. S. Jin, and J. Ye, Nature **501**, 521 (2013).
[36] L. Anderegg, L. W. Cheuk, Y. Bao, S. Burchesky, W. Ketterle, K.-K. Ni, and J. M. Doyle, Science **365**, 1156 (2019), https://science.sciencemag.org/content/365/6458/1156.full.pdf.
[37] S. Braun, J. P. Ronzheimer, M. Schreiber, S. S. Hodgman, T. Rom, I. Bloch, and U. Schneider, Science **339**, 52 (2013).
[38] T. Müller, S. Fölling, A. Widera, and I. Bloch, Phys. Rev. Lett. **99**, 200405 (2007).
[39] G. Wirth, M. Ölschläger, and A. Hemmerich, Nature Physics **7**, 147 (2011).
[40] In 1D and 2D, it may be possible to place $S$ and $B$ "side-by-side," so that their contact scales extensively with their volume. This arrangement could reduce the equilibration time, since one no longer requires diffusion. However, the coupling between $S$ and $B$ now has a non-trivial contribution to the thermodynamics and its effect would have to be accounted for in detail.
[41] F. D. M. Haldane, Phys. Rev. Lett. **50**, 1153 (1983).

[42] I. Affleck, T. Kennedy, E. H. Lieb, and H. Tasaki, Phys. Rev. Lett. **59**, 799 (1987).

[43] C. Senko, P. Richerme, J. Smith, A. Lee, I. Cohen, A. Retzker, and C. Monroe, Phys. Rev. X **5**, 021026 (2015).

[44] See supplementary information.

[45] K. Damle and S. Sachdev, Phys. Rev. B **57**, 8307 (1998).

[46] J. Karadamoglou and X. Zotos, Physical review letters **93**, 177203 (2004).

[47] G. Vidal, Phys. Rev. Lett. **91**, 147902 (2003).

[48] We work at $\gamma = \frac{3}{4}$, which reduces the correlation length relative to $\gamma = 0$ but is otherwise completely generic.

[49] Note that while this state seems contrived from an experimental perspective, it is convenient to prepare numerically, and owing to ergodicity the only relevant characteristic is its energy density.

[50] W. Hofstetter, J. I. Cirac, P. Zoller, E. Demler, and M. Lukin, Phys. Rev. Lett. **89**, 220407 (2002).

[51] R. A. Hart, P. M. Duarte, T.-L. Yang, X. Liu, T. Paiva, E. Khatami, R. T. Scalettar, N. Trivedi, D. A. Huse, and R. G. Hulet, Nature (London) **519**, 211 (2015), arXiv:1407.5932.

[52] A.-M. Daré, L. Raymond, G. Albinet, and A.-M. Tremblay, Physical Review B **76**, 064402 (2007).

[53] C. Karrasch, J. H. Bardarson, and J. E. Moore, New Journal of Physics **15**, 083031 (2013).

[54] B. Yan, S. A. Moses, B. Gadway, J. P. Covey, K. R. Hazzard, A. M. Rey, D. S. Jin, and J. Ye, Nature **501**, 521 (2013).

[55] J. Zeiher, R. van Bijnen, P. Schauß, S. Hild, J.-y. Choi, T. Pohl, I. Bloch, and C. Gross, arXiv preprint arXiv:1602.06313 (2016).

[56] J. Smith, A. Lee, P. Richerme, B. Neyenhuis, P. W. Hess, P. Hauke, M. Heyl, D. A. Huse, and C. Monroe, arXiv preprint arXiv:1508.07026 (2015).

[57] E. A. Martinez, C. Muschik, P. Schindler, D. Nigg, A. Erhard, M. Heyl, P. Hauke, M. Dalmonte, T. Monz, P. Zoller, *et al.*, arXiv preprint arXiv:1605.04570 (2016).

[58] We note that in our TEBD studies, we have focused on models with short-range interactions owing to numerical tractability. One might wonder whether long-range interactions still allow for a clear distinction between the system and bath regions. Crucially, the ability to distinguish between the system and bath in the thermodynamic limit does not require a strictly short-range interaction, only that the interfacial contribution to the free energy scales with the interfaces' area rather than with the volume of the bulk. For example, for a $1/R^\alpha$ power-law interactions in $d$-dimensions, degrees of freedom interact with a net strength of $R^{d-1-\alpha}$ with degrees of freedom at distance $R$. Thus, this condition is naturally satisfied if $\alpha + 1 > d$, which is the case for both dipolar molecules ($\alpha = 3$) and Rydberg arrays ($\alpha = 6$).

[59] A. V. Gorshkov, S. R. Manmana, G. Chen, J. Ye, E. Demler, M. D. Lukin, and A. M. Rey, Phys. Rev. Lett. **107**, 115301 (2011).

[60] N. Y. Yao, M. P. Zaletel, D. M. Stamper-Kurn, and A. Vishwanath, arXiv preprint arXiv:1510.06403 (2015).

[61] D. S. Fisher, Physical Review B **50**, 3799 (1994).

[62] A. Keesling, A. Omran, H. Levine, H. Bernien, H. Pichler, S. Choi, R. Samajdar, S. Schwartz, P. Silvi, S. Sachdev, *et al.*, Nature **568**, 207 (2019).

[63] S. de Léséleuc, V. Lienhard, P. Scholl, D. Barredo, S. Weber, N. Lang, H. P. Büchler, T. Lahaye, and A. Browaeys, Science **365**, 775 (2019), https://science.sciencemag.org/content/365/6455/775.full.pdf.

[64] A. Browaeys and T. Lahaye, Nature Physics **16**, 132 (2020).

[65] M. Endres, H. Bernien, A. Keesling, H. Levine, E. R. Anschuetz, A. Krajenbrink, C. Senko, V. Vuletic, M. Greiner, and M. D. Lukin, Science **354**, 1024 (2016), http://science.sciencemag.org/content/354/6315/1024.full.pdf.

[66] D. Barredo, S. de Léséleuc, V. Lienhard, T. Lahaye, and A. Browaeys, Science **354**, 1021 (2016), http://science.sciencemag.org/content/354/6315/1021.full.pdf.

[67] D. Barredo, V. Lienhard, S. de Léséleuc, T. Lahaye, and A. Browaeys, Nature **561**, 79 (2018).

[68] R. Samajdar, W. W. Ho, H. Pichler, M. D. Lukin, and S. Sachdev, Physical Review Letters **124**, 103601 (2020).

[69] R. L. Sugar, D. J. Scalapino, S. R. White, E. Y. Loh, and R. Scalettar, "Quantum electron simulation toolbox," .

[70] P. Medley, D. M. Weld, H. Miyake, D. E. Pritchard, and W. Ketterle, Phys. Rev. Lett. **106**, 195301 (2011).

[71] M. J. Ku, A. T. Sommer, L. W. Cheuk, and M. W. Zwierlein, Science **335**, 563 (2012).

[72] P. Debye, Annalen der Physik **386**, 1154 (1926).

[73] W. F. Giauque, Journal of the American Chemical Society **49**, 1864 (1927), http://dx.doi.org/10.1021/ja01407a003.